Enabling Wideband Full-Duplex Wireless via Frequency-Domain Equalization

ACM MobiCom 2019 SRC Winner – First Place (Graduate)*

Tingjun Chen
Department of Electrical Engineering, Columbia University
http://www.columbia.edu/~tc2668
tingjun@ee.columbia.edu

ABSTRACT

Full-duplex (FD) wireless can significantly enhance spectrum efficiency but requires tremendous amount of self-interference (SI) cancellation. Recent advances in the RFIC community enabled wideband RF SI cancellation in *integrated circuits (ICs)* via frequency-domain equalization (FDE) using reconfigurable RF filters, which *can be realized in small-form-factor devices*. In this work, we present the design and optimization of an FDE-based RF canceller implemented on a printed circuit board (PCB), which emulates its RFIC counterpart. We perform extensive evaluations of the FDE-based FD radios using a software-defined radio (SDR) testbed in different network settings. Experiments show that it achieves 95 dB overall SI cancellation (52 dB in the RF domain) across 20 MHz bandwidth, and an average link-level FD gain of 1.87×. We also conduct unique experiments in: (i) uplink-downlink networks with inter-user interference, and (ii) heterogeneous networks with half-duplex and FD users. The experimental FD gains in the two types of networks confirm previous analytical results. They depend on the users' SNR values and the number of FD users, and are 1.14×–1.25× and 1.25×–1.73×, respectively. Finally, we describe the integration of the FD radios in the city-scale NSF PAWR COSMOS advanced wireless testbed and the associated two pilot COSMOS experiments: (i) the first remotely accessible experiment on open-access FD wireless, and (ii) converged optical-wireless networking with FD and edge cloud.

1 INTRODUCTION

Wireless technology has evolved at a remarkable rate, with data rates increasing by four orders of magnitude over the past twenty years [4, 7]. The push towards 5G will continue this trend, with radio access links soon operating at 1 Gbps or higher [9, 12], and access network latency reduced from 10s of milliseconds to the order of 1 ms [3, 15]. Such capabilities are required to enable a broad new class of real-time applications including augmented/virtual reality (AR/VR) and cloud-based autonomous vehicles.

*This SRC submission corresponds to a paper that appeared in Proc. ACM MobiCom'19 [6] along with a poster presentation at ACM MobiCom'19.

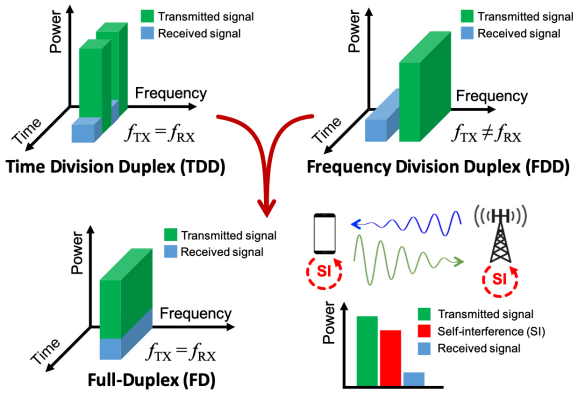

Figure 1: **Full-duplex (FD) wireless: simultaneous transmission and reception at the same frequency, where strong self-interference (SI) needs to be cancelled to below the radio noise floor.**

Full-duplex (FD) wireless – simultaneous transmission and reception on the same frequency channel (see Fig. 1) – is an emerging communication paradigm that can significantly improve spectrum efficiency at the physical layer and provide many other benefits at the higher layers of the networking stack [14, 17]. The main challenge associated with FD is the extremely strong self-interference (SI) signal that needs to be suppressed, requiring 90–110 dB of SI cancellation.

Fig. 2(a) depicts the block diagram of an FD radio that incorporates SI suppression at the antenna interface, and SI cancellation in analog/RF and digital domains. Recent work using off-the-shelf components and software-defined radios (SDRs) has established the feasibility of FD wireless [5, 8, 10]. However, RF cancellers achieving wideband SI cancellation (e.g., [5, 10]) rely on transmission-line delays, which cannot be realized in small-form-factor nodes and/or integrated circuits (ICs). This is due to the required length for generating nanosecond-scale time delays (e.g., 10s of centimeters) and the lossy nature of the silicon substrate.

A *compact IC-based* design is necessary for supporting FD in hand-held devices [16, 17]. Recent advances in the RFIC community allowed achieving wideband RF SI cancellation in ICs based on the technique of frequency-domain equalization (FDE) [16]. In contrast to the delay line-based

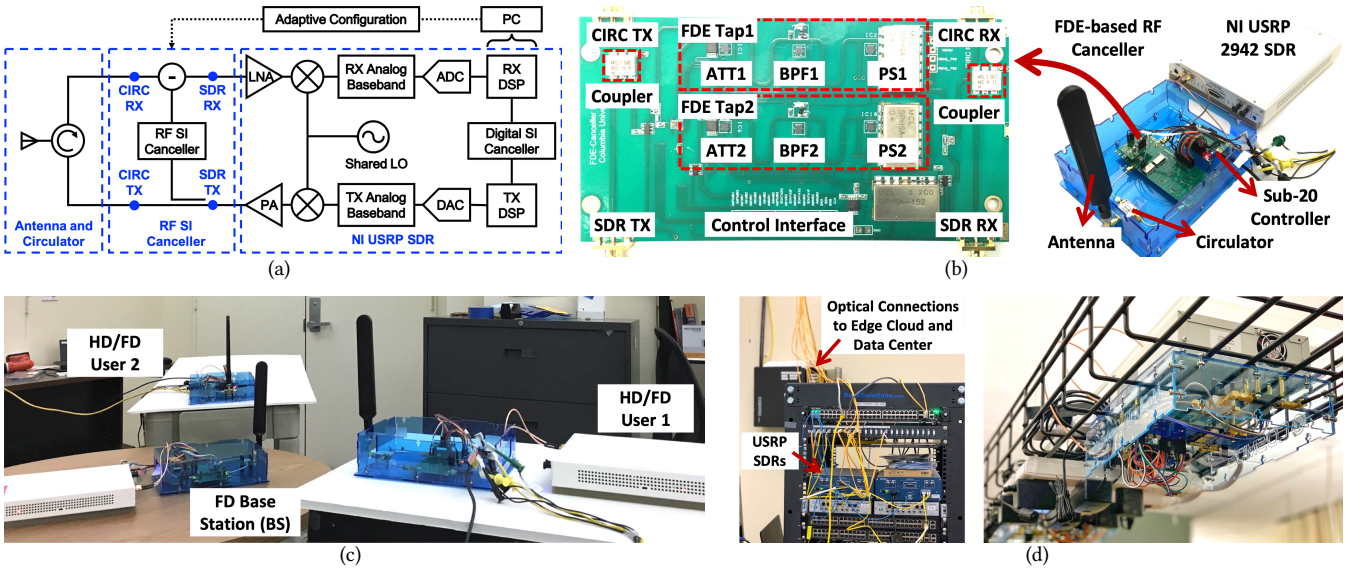

Figure 2: **(a) Block diagram of a full-duplex (FD) radio featuring self-interference (SI) suppression/cancellation at the antenna interface, and in the RF and digital domains, (b) the implemented wideband FD radio based on frequency-domain equalization (FDE), (c) our experimental testbed consisting of both half-duplex (HD) and FD nodes, and (d) sandbox 2 of the city-scale NSF PAWR COSMOS advanced wireless testbed (located at Columbia University) and the integrated world's first open-access wideband FD radios which are remotely accessible.**

approaches (i.e., time-domain equalization), the FDE-based RF canceller utilizes reconfigurable 2nd-order bandpass filters (BPFs) with high quality factors to emulate the frequency-selective antenna interface. While major advances have been made at the IC level (e.g., [16]), there is still a need to: *(i) understand the fundamental limits of the achievable RF SI cancellation based on the technique of FDE, (ii) develop efficient and adaptive configuration schemes for this new type of RF canceller, and (iii) evaluate the system-level performance of such IC-based FD radios in different network settings.*

Since interfacing an RFIC canceller with an SDR presents numerous technical challenges, in this work, we designed and implemented an FDE-based RF canceller using discrete components on a printed circuit board (PCB) with more stable and robust performance (more details can be found in [6]). Using the PCB canceller, which emulates its RFIC counterpart and facilitates the evaluation of the canceller configuration scheme, we prototyped FDE-based wideband FD radios on an SDR platform (see Fig. 2(b)). We also implemented a unique testbed consisting of multiple FD nodes for experimentation at the link- and network-level (see Fig. 2(c)). For example, our FDE-based FD radio achieves an average FD link throughput gain of 1.85–1.91×.

In this work, we present the design, optimization, and experimentation of FDE-based FD radios. To the best of our knowledge, this is the *first* thorough study of wideband RF SI cancellation achieved via a frequency-domain-based approach (which is suitable for compact implementations) that is grounded in real-world implementation and includes extensive system- and network-level experimentation.

Moreover, despite extensive research in this area, an open-access wireless testbed with FD-capable nodes is still needed for experimental evaluations of FD-related algorithms at the higher layers. To allow the broader community to experiment with FD, we integrated the FDE-based FD radios in the NSF PAWR COSMOS testbed [13] (see Fig. 2(d)), which is a programmable city-scale advanced wireless testbed being deploying in West Harlem, New York City. These are the *world's first open-access wideband FD radios that are remotely accessible.* We present the integration of FDE-based FD radios in COSMOS and the associated two *first-of-their-kind* experiments: (i) open-access FD wireless, and (ii) converged optical-wireless networking with FD and edge cloud.

2 FDE-BASED RF CANCELLER AND FD RADIO: DESIGN & IMPLEMENTATION

In this section, we briefly describe the FDE-based RF canceller, and the prototyped FDE-based FD radios and testbed (for more details, please see [6]).

FDE-based PCB Canceller Implementation. Fig. 2(b) shows the implemented PCB canceller with 2 FDE taps, which is optimized around 900 MHz operating frequency. In particular, a reference signal is tapped from the SDR TX output and is split into 2 FDE taps. Then, the signals after each FDE tap are combined and RF SI cancellation is performed at the SDR RX input. Each FDE tap consists of a reconfigurable 2nd-order BPF with high quality factor as well as an attenuator and phase shifter for amplitude and phase controls, respectively. The BPF center frequency can be adjusted through the capacitor in the RLC resonance tank. In order to achieve a high

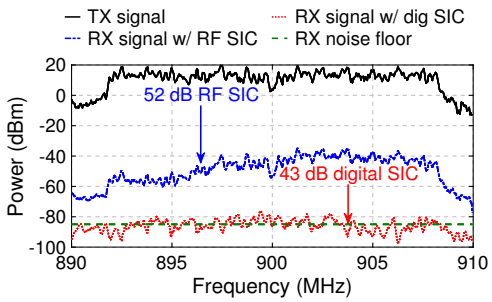

Figure 3: **Power spectrum of the received signal after SI cancellation (SIC) in the RF and digital domains with +10 dBm average TX power, 20 MHz bandwidth, and −85 dBm RX noise floor.**

and tunable BPF quality factor, impedance transformation networks including digitally tunable capacitors are introduced. The programmable attenuator has a tuning range of 0–15.5 dB with a 0.5 dB resolution, and the passive phase shifter is controlled by an 8-bit digital-to-analog converter (DAC) and covers full 360° range.

FDE-based PCB Canceller Model. To allow for efficient and adaptive canceller configuration, we derive a realistic model for the frequency response of the PCB canceller using the transmission matrix theory. This model is validated through extensive measurements and shown to have high accuracy (i.e., the maximum amplitude/phase error is only 1.5 dB/12°).

Optimized Canceller Configuration. We developed and implemented a general FDE-based canceller configuration scheme that jointly optimizes all the FDE taps (for details see [6]). The inputs to the configuration scheme include: (i) the derived and validated PCB canceller model, (ii) the real-time SI channel (i.e., frequency response of the antenna interface) measured using a packet preamble (2 OFDM symbols), and (iii) the desired RF SI cancellation bandwidth. The canceller configuration scheme is implemented on the host PC, where the the PCB canceller response is pre-computed and stored for computational efficiency. In particular, the optimized PCB canceller configuration is obtained by solving a minimum mean square error problem followed by a finer-grained local search to achieve the best RF SI cancellation performance. This process can be done in <10 ms on a regular PC with quad-core Intel i7 CPU via a non-optimized MATLAB solver.

FDE-based FD Radio and Testbed using an SDR Platform. Figs. 2(b) and 2(c) depict our implemented FDE-based FD radios and testbed using SDRs. In particular, each FD radio consists of an antenna, a coaxial circulator, an FDE-based RF canceller, a USRP SDR, and a compute node, and operates at around 900 MHz carrier frequency.

We implemented a full OFDM-based PHY layer with a real-time RF bandwidth of 20 MHz using NI LabVIEW, supporting various modulation and coding schemes (MCSs) from BPSK-1/2 to 64QAM-3/4. The digital SI cancellation algorithm based on Volterra series with a highest non-linearity order of 7

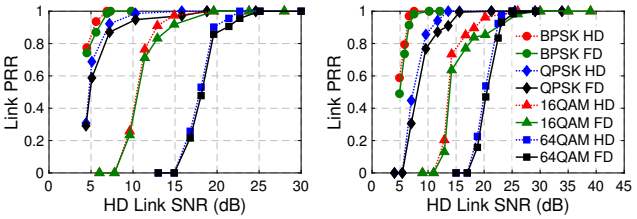

Figure 4: **HD and FD link packet reception ratio (PRR) with varying HD link SNR and MCSs: (left) coding rate 1/2, (right) coding rate 3/4.**

is also implemented in LabVIEW to further suppress the residual SI signal after RF SI cancellation.

Fig. 3 shows the measurement results of the FDE-based FD radio achieving 95 dB overall SI cancellation across 20 MHz (52/43 dB in the RF/digital domain). Since the USRP has a noise floor of −85 dBm (limited by the environmental interference at around 900 MHz), the FD radio can support a maximum average TX power of +10 dBm (a peak TX power of +20 dBm). In total, our testbed consists of 3 FDE-based FD radios and regular USRPs without the PCB canceller.

3 EXPERIMENTAL EVALUATION

In this section, we present experimental evaluation of the FDE-based FD radios at the link and network levels.

Link-Level: SNR-PRR Relationship and FD Gains. We first evaluate the relationship between link signal-to-noise ratio (SNR) and packet reception ratio (PRR) using two FDE-based FD radios, where data packets are sent over the wireless link simultaneously in FD mode or in alternating directions in half-duplex (HD) mode (i.e., the two radios take turns and transmit to each other). In each experiment, both radios send a sequence of 50 OFDM streams, each OFDM stream contains 20 800-Byte OFDM packets.

Fig. 4 shows the relationship between link PRR and HD link SNR with varying MCSs. The results show that with sufficient link SNR values (e.g., 28 dB for 64QAM-3/4), the FDE-based FD radio achieves a link PRR of 100%. With insufficient link SNR values, the average FD link PRR is 6.5% lower than the HD link PRR across varying MCSs. Since packets are sent simultaneously in both directions on an FD link, *this average PRR degradation is equivalent to an average FD link throughput gain of 1.87× under the same MCS.*

We also conduct experiments in both line-of-sight (LOS) and non-line-of-sight (NLOS) settings on a 45 m × 20 m floor, and measure the HD (resp. FD) link throughput. The FD gain is then computed as the ratio between FD and HD throughput values. Fig. 5 shows the average HD and FD link throughput with 16QAM-3/4 and 16QAM-3/4 MCSs. The results show that with sufficient link SNR values, *the FDE-based FD radios achieve an* exact *link throughput gain of 2× with a link PRR of 1.* With medium link SNR values, where the link PRR less than 1, the average FD link throughput gains across varying MCSs are 1.91/1.85× for the LOS/NLOS experiments.

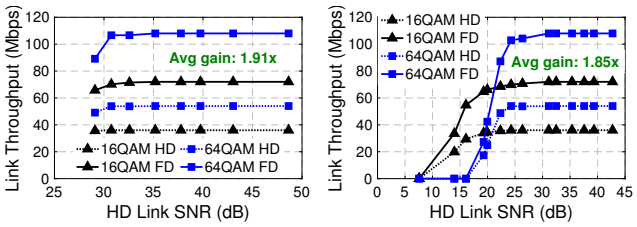

Figure 5: **HD and FD link throughput in the LOS (left) and NLOS (right) experiments with 16QAM-3/4 and 64QAM-3/4 MCSs.**

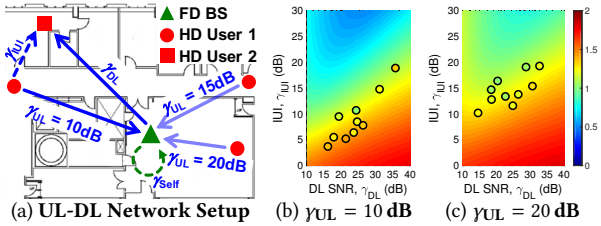

(a) **UL-DL Network Setup** (b) $\gamma_{\text{UL}} = 10$ **dB** (c) $\gamma_{\text{UL}} = 20$ **dB**

Figure 6: **(a) Experimental setup for uplink-downlink (UL-DL) networks, and (b)–(c) analytical (colored surface) and experimental (filled circles) network-level FD throughput gains with UL SNR values of $\gamma_{\text{UL}} \in \{10, 20\}$ dB.**

Network-Level FD Gains. We experimentally evaluate the network-level FD throughput gains and compare to corresponding analytical results (e.g., [11]). We consider two types of networks: (i) *uplink-downlink (UL-DL) networks* with one FD base station (BS) and two HD users with inter-user interference (IUI), and (ii) *heterogeneous HD-FD networks* with both HD and FD users.

(i) UL-DL Networks with IUI. We use γ_{UL}, γ_{DL}, and γ_{IUI} to denote the UL SNR, DL SNR, and level of IUI, respectively. Fig. 6 shows the analytical (colored surface) and experimental (filled circles) FD gains. It can be seen that smaller values of γ_{UL} and lower ratios between γ_{DL} and γ_{IUI} lead to higher FD gains in both analysis and experiments, and the average experimental FD gains are 1.25/1.16/1.14× for $\gamma_{\text{UL}} = 10/15/20$ dB. Overall, *the average experimental FD gain is 93% of the analytical FD gain*, which confirms the analysis in [11] and demonstrate practical FD gains in wideband UL-DL networks without changing the current network stack (i.e., only bringing FD capability to the BS). Moreover, performance improvements are expected through advanced power control and scheduling schemes.

(ii) Heterogeneous 4-Node Networks. We also experimentally study 4-node networks (e.g., see Fig. 7(a)) where zero, one, and two users are FD-capable. Fig. 7(b) shows the CDF of the experimental FD throughput gains with measured link SNR between 5–45 dB. Overall, the median network throughput is increased by 1.25/1.52× when one/two users become FD-capable. The trend shows that in real-world environments, the network throughput increases as more users become FD-capable, and the improvement is more significant with higher user SNR values.

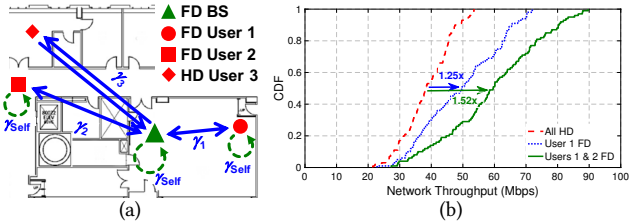

(a) (b)

Figure 7: **(a) Experimental setup for heterogeneous 4-node networks, and (b) CDF of experimental network-level FD throughput gains when zero, one, or two users are FD-capable.**

4 OPEN-ACCESS FD WIRELESS IN THE CITY-SCALE COSMOS TESTBED

COSMOS – **C**loud enhanced **O**pen **S**oftware defined **MO**bile wireless *testbed* for city-**S**cale deployment – is an advanced wireless testbed [13] which is being deployed in West Harlem, New York City, as part of the NSF Platforms for Advanced Wireless Research (PAWR) program. It will enable researchers to explore the technology "sweet spot" of ultra-high bandwidth, ultra-low latency, and edge computing in the most demanding real-world environment. In order to support accurate experiments over a broad range of new system designs, COSMOS incorporates emerging spectrum techniques for Gbps+ radio access such as millimeter-wave (mmWave) and FD wireless, low latency mobile core networks, and edge cloud.

We design and conduct several example experiments to drive and validate various capabilities of the COSMOS testbed. In particular, two first-of-their-kind COSMOS pilot experiments, described below, are based on the FDE-based wideband FD radios. We also believe that these examples can help researchers envision and plan their own experiments.

Experiment 1: Open-Access FD Wireless. As described in Section 1, despite extensive research in the area of FD wireless, an open-access wireless testbed with FD-capable nodes is crucial for experimental evaluations of FD-related algorithms at different layers of the networking stack. To allow the broader community to experiment with open-access FD wireless, following our integration of the *narrowband* FD radio in the ORBIT wireless testbed, we recently integrated the FDE-based *wideband* FD radios in sandbox 2 of the COSMOS advanced wireless testbed (see Fig. 2(d) and [2]).

In order to achieve a fully open-source design with easy access, our software implementation is built on the free GNU Radio development platform. We also provide several example baseline programs and FD experiments, which include: (i) a software-based SI channel measurement toolkit, (ii) a customized control module for RF canceller configuration, and (iii) a real-time FD link demonstration with packet-level digital SI cancellation and packet decoding. Advanced example experiments at the higher layers are also under development. The detailed design and schematics of an improved version of the FDE-based RF canceller are made available to the public.

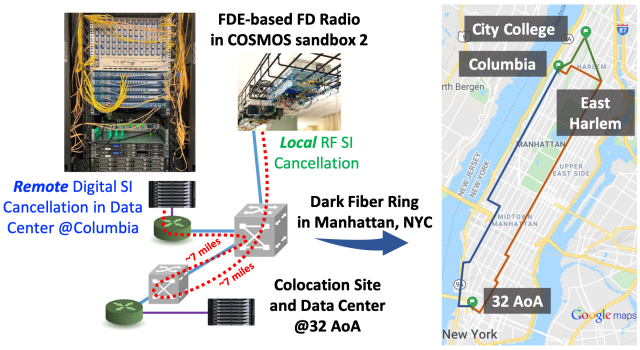

Figure 8: **FDE-based wideband FD radios integrated with the COSMOS optical x-haul network (including dark fiber deployed in Manhattan, New York City), which demonstrates the cloud radio access network (C-RAN) architecture with edge cloud capabilities.**

Experiment 2: FD Wireless with Edge Cloud. Another example experiment is on converged optical-wireless x-haul networking, which demonstrates the cloud radio access network (C-RAN) architecture integrating radio resources and the optical transport network. The experimental setup is shown in Fig. 8. In particular, the FDE-based wideband FD radio, described above, serves as an FD BS located in the COSMOS sandbox 2. The BS sends 20 MHz baseband I/Q data (limited by the interface between the SDR and server) over the dark fiber (with 10/100 Gbps transceivers) to the optical switches at the remote data center of NYU at 32 Avenue of the Americas (AoA). The I/Q data is then sent back to the data center at Columbia for remote digital signal processing at ~14 miles away from the FD radio. This experiment evaluates the capability of integrating FD with an edge cloud using COSMOS' dark fiber network deployed in Manhattan, New York City. Due to its high capacity (10s of Gbps) and low latency (<1 ms), such an optical x-haul network can support high-performance computing tasks and flexible edge topologies.

5 CONCLUSION

We designed and implemented an FD radio using the FDE technique, which achieves wideband RF SI cancellation in compact nodes (details can be found in [6]). The FDE-based FD radios were evaluated using an SDR testbed with good performance at the node, link, and network levels. We integrated open-access FD radios in the COSMOS testbed and demonstrated two unique COSMOS pilot experiments with real-time FD wireless and edge cloud (tutorials and open-source code are available at [1]). Future directions include: (i) development and experimentation with resource allocation and scheduling algorithms tailored for FDE-based FD radios, and (ii) installation of wideband FD radios at various outdoor locations in COSMOS in order to support research community experimentation with FD in a dense urban area.

ACKNOWLEDGMENTS

This work was supported in part by NSF grants ECCS-1547406, CNS-1650685, CNS-1827923, a Facebook Fellowship, and a Wei Family Private Foundation Fellowship.

REFERENCES

[1] 2020. COSMOS tutorials. https://wiki.cosmos-lab.org/wiki/tutorials/.
[2] 2020. Tutorial: Full-duplex wireless in the COSMOS testbed. https://wiki.cosmos-lab.org/wiki/tutorials/full_duplex.
[3] Mamta Agiwal, Abhishek Roy, and Navrati Saxena. 2016. Next generation 5G wireless networks: A comprehensive survey. *Commun. Surveys Tuts.* 18, 3 (2016), 1617–1655.
[4] Jeffrey G Andrews, Stefano Buzzi, Wan Choi, Stephen V Hanly, Angel Lozano, Anthony CK Soong, and Jianzhong Charlie Zhang. 2014. What will 5G be? *IEEE J. Sel. Areas Commun.* 32, 6 (2014), 1065–1082.
[5] Dinesh Bharadia, Emily McMilin, and Sachin Katti. 2013. Full duplex radios. In *Proc. ACM SIGCOMM'13.*
[6] Tingjun Chen, Mahmood Baraani Dastjerdi, Jin Zhou, Harish Krishnaswamy, and Gil Zussman. 2019. Wideband full-duplex wireless via frequency-domain equalization: Design and experimentation. In *Proc. ACM MobiCom'19.*
[7] Cisco. 2018. The Zettabyte Era: Trends and Analysis. https://www.cisco.com/c/en/us/solutions/collateral/service-provider/global-cloud-index-gci/white-paper-c11-738085.html.
[8] Melissa Duarte and Ashutosh Sabharwal. 2010. Full-duplex wireless communications using off-the-shelf radios: Feasibility and first results. In *Proc. Asilomar Conference on Signals, Systems, and Computers.*
[9] Ericsson. 2016. 5G radio access. https://www.ericsson.com/assets/local/publications/white-papers/wp-5g.pdf.
[10] Dani Korpi, Joose Tamminen, Matias Turunen, Timo Huusari, Yang-Seok Choi, Lauri Anttila, Shilpa Talwar, and Mikko Valkama. 2016. Full-duplex mobile device: Pushing the limits. *IEEE Commun, Mag.* 54, 9 (2016), 80–87.
[11] Jelena Marasevic, Jin Zhou, Harish Krishnaswamy, Yuan Zhong, and Gil Zussman. 2017. Resource allocation and rate gains in practical full-duplex systems. *IEEE/ACM Trans. Netw.* 25, 1 (2017), 292–305.
[12] Qualcomm. 2018. 5G: The Fabric for Society. https://www.qualcomm.com/media/documents/files/5g-vision-use-cases.pdf.
[13] Dipankar Raychaudhuri, Ivan Seskar, Gil Zussman, Thanasis Korakis, Dan Kilper, Tingjun Chen, Jakub Kolodziejski, Michael Sherman, Zoran Kostic, Xiaoxiong Gu, Harish Krishnaswamy, Sumit Maheshwari, Panagiotis Skrimponis, and Craig Gutterman. 2020. Challenge: COSMOS: A City-Scale Programmable Testbed for Experimentation with Advanced Wireless. In *Proc. ACM MobiCom'20 (to appear).*
[14] Ashutosh Sabharwal, Philip Schniter, Dongning Guo, Daniel W Bliss, Sampath Rangarajan, and Risto Wichman. 2014. In-band full-duplex wireless: Challenges and opportunities. *IEEE J. Sel. Areas Commun.* 32, 9 (2014), 1637–1652.
[15] Mansoor Shafi, Andreas F Molisch, Peter J Smith, Thomas Haustein, Peiying Zhu, Prasan De Silva, Fredrik Tufvesson, Anass Benjebbour, and Gerhard Wunder. 2017. 5G: A tutorial overview of standards, trials, challenges, deployment, and practice. *IEEE J. Sel. Areas Commun.* 35, 6 (2017), 1201–1221.
[16] Jin Zhou, Tsung-Hao Chuang, Tolga Dinc, and Harish Krishnaswamy. 2015. Integrated wideband self-interference cancellation in the RF domain for FDD and full-duplex wireless. *IEEE J. Solid-State Circuits* 50, 12 (2015), 3015–3031.
[17] Jin Zhou, Negar Reiskarimian, Jelena Diakonikolas, Tolga Dinc, Tingjun Chen, Gil Zussman, and Harish Krishnaswamy. 2017. Integrated full duplex radios. *IEEE Commun. Mag.* 55, 4 (2017), 142–151.